Complex Formation of DNA with Oppositely Charged Polyelectrolytes of Different Chain Topology: Cylindrical Brushes and Dendrimers

Dominic Störkle, Sabrina Duschner, Nils Heimann, Michael Maskos, and Manfred Schmidt*

Institut für Physikalische Chemie, Universität Mainz, Jakob-Welder-Weg 11, D-55128 Mainz, Germany

Received May 24, 2007; Revised Manuscript Received July 23, 2007

ABSTRACT: The complex formation between DNA (pUC19-supercoiled DNA, 2686 base pairs) and some polycations of different chain topologies in aqueous solution was studied by light scattering, gel electrophoresis, and AFM. The investigated polycations comprised cylindrical brush polymers with quaternized poly(vinylpyridine) and polyethylene imine side chains as well as a fifth generation dendrimer thus covering a broad molar mass regime of 3×10^4 g mol^{-1} < M_w < 1×10^7 g mol^{-1} and very different chemical charges/molecule, Z^+, of 127 < Z^+ < 5500. Irrespective of the polycation, the complexes formed in dilute solution exhibited a similar size in terms of the mean square radius of gyration, $\langle R_g^2 \rangle$, i.e., 30 nm < R_g < 40 nm (excess of DNA) and 40 nm < R_g < 55 nm (excess of polycation). At a large excess of either DNA or polycation, the complexes were shown to coexist with the uncomplexed molecules of the excess component and did not vary in size with increasing weight fraction of the minority component. Only if the number of complexes became comparable to the number of uncomplexed molecules was inter complex bridging observed to occur, which eventually led to phase separation. The extremely large charge density mismatch between the DNA and the polycations caused strongly "overcharged" cationic complexes to be formed at excess polycation whereas at excess DNA a small anionic charge of the complexes was found. The results are explained qualitatively in terms of kinetically controlled complexation.

Introduction

The formation and structure of polyelectrolyte complexes have been subject of numerous investigations since a long time.[1,2] Besides the investigation of complexes formed by oppositely charged flexible coils[3−6] also complexes containing semiflexible DNA were intensively studied,[7−32] in order to elucidate the phenomenon of DNA condensation and to optimize encapsulation of DNA for gene transfection. Remarkably, little is known of how complex formation, i.e., the size and the structure of the complexes, is governed by the chain stiffness and by the chain topology of the polycations utilized, except for some indirect evidence for dendrimers of various generations[33−37] and for colloids of different size.[38,39] Only one report is published on the complex formation of DNA with a charged cylindrical polymer, i.e., a polymer densely grafted with second to fourth generation dendrons.[40,41]

Some contradictory postulations exist in the literature concerning the thermodynamic state of the complexes. It is not entirely clear under which experimental conditions (i) the complex formation is kinetically controlled leading to irreversibly frozen, nonequilibrium structures or (ii) reversible complex formation occurs upon changing, for instance, concentration and/or ionic strength, or (iii) the complexes are formed at thermodynamic equilibrium. The latter was postulated to occur at high ionic strength, i.e., above 0.1 M added salt.[3]

The present work addresses in some detail the condensation and encapsulation of DNA by polycations of novel chain topologies, i.e., cylindrical brush polymers, with different side chain lengths and charge densities.[42] A commercial fifth generation PAMAM dendrimer serves as reference.

* Corresponding author. E-mail: mschmidt@uni-mainz.de.

Experimental Section

Materials. Sodium phosphate monobasic dihydrate extra pure (Merck), sodium phosphate dibasic 99.95% (Aldrich), magnesium chloride hexahydrate extra pure (Merck), agarose (Sigma), and TBE buffer (10×, Amersham) were used as received. For all experiments the polymers were dissolved in 5 mM sodium phosphate buffer (pH = 7) unless otherwise noted.

pUC19-Supercoiled DNA. The pUC19-supercoiled DNA (Elim-Biopharmaceuticals) was used as received. The degree of supercoiling was higher than 90% as specified by the supplier. pUC19 DNA contains 2686 base pairs and has a theoretical molar mass of 1.66 e6 g mol^{-1}. Static light scattering in 5 mM sodium phosphate buffer (pH = 7) yields the theoretical molar mass assuming dn/dc = 0.17 mL g^{-1} according to the literature.[43,44] The characterization of the used pUC19-supercoiled DNA by static and dynamic light scattering is summarized in Table 1; a typical Berry plot is shown in the Supporting Information.

PVP26 and PVP47 Cylindrical Brush Polymers. The synthesis of the polymacromonomers (cylindrical brushes) containing 2-vinylpyridine side chains, which are quaternized with ethyl bromide, is described elsewhere.[42] In this study, two brushes with a side chain degree of polymerization of 25.5 (PVP26) and 46.7 (PVP47) were utilized. The degree of quaternization was determined by elemental analysis to 47% and 52% respectively. The light scattering characterization of PVP26 and PVP47 is summarized in Table 1.

PEI Cylindrical Brush Polymer. First poly(*N*-benzoyl ethylene imine)-macromonomers were synthesized according to Gross et al.[45] (MALDI−TOF-characterization: M_n = 4290 g mol^{-1}, M_w/M_n = 1.04, P_n = 28). These macromonomers were polymerized by radical polymerization in *N*-methylpyrrolidone with AIBN for 10 days at 58 °C to polymacromonomers which are known to adopt the shape of cylindrical brushes (light scattering characterization in chloroform: $M_w = 1.47 \times 10^6$ g mol^{-1}, dn/dc = 0.145 mL g^{-1}, R_g = 26.7 nm, R_h = 18.6 nm). Subsequent hydrolysis according to Tanaka[46] resulted in cylindrical brush molecules with PEI side chains. The hydrolysis was quantitative within experimental error. After freeze-drying from 10 wt % HCl, the hydrochloride of the

10.1021/ma0711689 CCC: $37.00
Published on Web 10/05/2007

Table 1. Light Scattering Characterization of the Investigated Polymers

polymer	solvent	(dn/dc)/mL g^{-1}	M_w/g mol^{-1}	A_2/mol mL g^{-2}	R_g/nm	R_h/nm	R_g/R_h
pUC19	5 mM phosphate buffer	0.17[a]	1.7×10^6	6.7×10^{-4}	65.6	43.6	1.5
PVP26	aq 10 mM NaBr	0.178[b]	10.1×10^6	~0	87.2	48.2	1.8
PVP47	5 mM phosphate buffer	0.178[c]	3.7×10^6	1.2×10^{-5}	45.8	33.1	1.4
PEI*HCl	aq 0.1 M HCl	0.20[a]	1.2×10^6 [e]	1.1×10^{-4}	46.8	26.5	1.8
PAMAM-G5	MeOH +10 mM LiBr	0.230[d]	2.8×10^4	5×10^{-4}		3.4	

[a] Literature value. [b] Determined experimentally in dialysis equilibrium, this work. [c] Assumed to be identical to PVP26 in 10 mM NaBr solution. [d] Determined experimentally, no dialysis equilibrium, this work. [e] Slightly aggregated: Theoretical value from the protected precursor chains: $M_w = 8.3 \times 10^5$ g/mol.

PEI brushes (PEI·HCl) was isolated, which constitutes the reference for the mass concentration in solution for this sample throughout this paper. The characterization of PEI·HCl brushes in 0.1 M aqueous HCl solution gives a weight-average molar mass of $M_w = 1.19 \times 10^6$ g mol^{-1} utilizing a literature value for (dn/dc) = 0.20 mL g^{-1}.[47,48] The molar mass is 40% higher than the theoretical molar mass $M_w = 8.28 \times 10^5$ g mol^{-1} calculated from the molar mass of the protected precursor polymer. In addition also R_g and R_h increased from 26.7 to 45.8 nm and 18.6 to 26.5 nm, respectively. Obviously the PEI brushes form some aggregates in aqueous solution, the extent of which decreases with time (time scale of several months). That means that the aggregation is caused by physical factors and not by chemical cross-linking. For the experiments in this paper, only freshly prepared PEI-brush solutions were used, in order to guarantee always the same degree of aggregation. The light-scattering results are included in Table 1.

PAMAM-G5 Dendrimer. The PAMAM-G5 dendrimer (Aldrich, produced by Dendritech, Midland) was received as a methanolic solution and used without further treatment. The concentration of the dendrimer in solution was determined by freeze-drying the dendrimer from water and subsequent drying in vacuum with KOH powder to constant weight. For the determination of the absolute molar mass, the refractive index increment and static light scattering were measured in methanol containing 10 mM LiBr yielding (dn/dc) = 0.23 mL g^{-1} and $M_w = 28\,000$ g mol^{-1}. Although the latter is close to the theoretical molar mass of the perfect dendrimer, $M_w = 28\,824$ g mol^{-1}, this coincidence might be misleading, because the G5-PAMAM dendrimers might be far from being perfect. Since the dendrimers are delivered in methanolic solution a somewhat uncertain concentration and possible filtration losses may introduce significant errors to the light scattering value which, however, would not seriously alter the conclusions of the present paper. The light scattering results are included in Table 1.

Since complex formation was performed in 5 mM phosphate buffer additional light scattering measurements for PVP26, PEI, and PAMAM-G5 dendrimers were also conducted in the phosphate buffer. Although the interpretation of the data was more complex similar results were obtained within experimental error.

Complex Preparation. For all complexation experiments, DNA and the respective polycations were dissolved in 5 mM sodium phosphate buffer (pH = 7) at a concentration of 2.5 mg L^{-1} unless stated otherwise. The minority component was always dropped into the solution containing the excess component covering a weight fraction of DNA of $0.05 \le w_{DNA} \le 0.95$ in increments of 0.05. w_{DNA} is defined as

$$w_{DNA} = \frac{m_{DNA}}{m_{DNA} + m_{polycation}} \quad (1)$$

The exact mixing ratio was determined by weighing the amount of added solution. Then, 30 s after each addition, the solution was gently shaken for approximately 1 min. Longer or more intensive shaking did not yield different results. For light scattering the complexes were prepared in dust-free 20 mm diameter quartz cuvettes (Hellma) by mixing the prefiltered DNA and respective polycation solutions in order to avoid filtration of the complexes, which could lead to concentration losses.

Measurements. AFM. For sample preparation, 10 μL of the desired complex solution was mixed with 2.5 μL of 10 mM $MgCl_2$. After 2−3 min, the whole solution was placed on freshly cleaved mica for another 2−3 min, followed by rinsing with Milli-Q water and drying with nitrogen. For imaging a Multimode AFM instrument (Nanoscope IIIa instrument, Digital Instruments, Santa Barbara, CA) in the tapping mode was used.

Agarose Gel Electrophoresis. The agarose gel electrophoresis was carried out with a PerfectBlue Horizontal Maxi Electrophoresis System, model Maxi M, and an E-Box-1000/20 M-gel imaging system (peqlab, Erlangen, Germany). The samples for gel electrophoresis (35 μL) were mixed with 15 μL of gel-loading buffer containing 0,1 M disodium EDTA and 40 w.-% sucrose (the exact content/concentration of sample in the loaded solution was determined by weight), loaded on the gel and run for about 1.5 h at 100 mA. The measurements comprise pure DNA in different concentrations for intensity calibration and the complex solutions. Additionally, identical samples of pure DNA (referred to as standard) were loaded on the gel in a defined grid for image analysis (background subtraction). A typical gel picture after ethidium bromide staining is shown in Figure 1a. By analyzing the digital images of the gels with Scion image (Scion Corporation, Frederick, MD) the intensity of the bands of supercoiled DNA (scDNA) were determined. From these the intensity relative to the standard (of the respecting lane) was calculated for each sample loaded on the gel.

For calibration, the relative intensities of the pure DNA samples were plotted as a function of DNA concentration and fitted by linear regression (see Figure 1b), which was utilized for the determination of free DNA in the complex solutions.

Static and Dynamic Light Scattering. Static light scattering (SLS) measurements were performed with an ALV−SP86 goniometer, an ALV-3000 correlator, a Uniphase HeNe Laser (25 mW output power at $\lambda = 632.8$ nm wavelength) and ALV/High QE APD avalanche diode fiber optic detection system. For dynamic light scattering (DLS), an ALV−SP125 goniometer, an ALV-5000 correlator, and a Spectra Physics 2060 argon ion laser (500 mW output power at $\lambda = 514.5$ nm wavelength) were utilized. The scattered intensity was divided by a beam splitter (approximately 50:50), each portion of which was detected by a photomultiplier. The two signals were cross-correlated in order to eliminate nonrandom electronic noise.

The complex solutions were typically measured from 30 to 150° in steps of 5° (SLS) or in steps of 10° (DLS). The static scattering intensities were analyzed according to standard procedures in order to yield the weight-average molar mass, M_w, and the mean square radius of gyration, $R_g = \sqrt{\langle R_g^2 \rangle_z}$. The correlation functions showed a monomodal decay and were fitted by a sum of two exponentials, from which the first cumulant Γ was calculated. The z-average diffusion coefficient D_z was obtained by extrapolation of Γ/q^2 for to $q = 0$ leading to the inverse z-average hydrodynamic radius $R_h = \langle R_h^{-1} \rangle_z^{-1}$ by formal application of Stokes law. Prior to mixing the homopolymer solutions were filtered through 0.2 μm pore size Dimex filters (Millipore LG) into 20 mm diameter quartz cuvettes (Hellma). The refractive index increment at $\lambda = 632.8$ nm wavelength was measured by a home-built Michelson interferometer as described elsewhere.[49]

Results and Discussions

Many, if not all polyelectrolyte complexes formed by highly charged polyions in aqueous solution of low ionic strength constitute kinetically frozen rather than equilibrium structures. Thus, the formation of the complexes depends on the concentra-

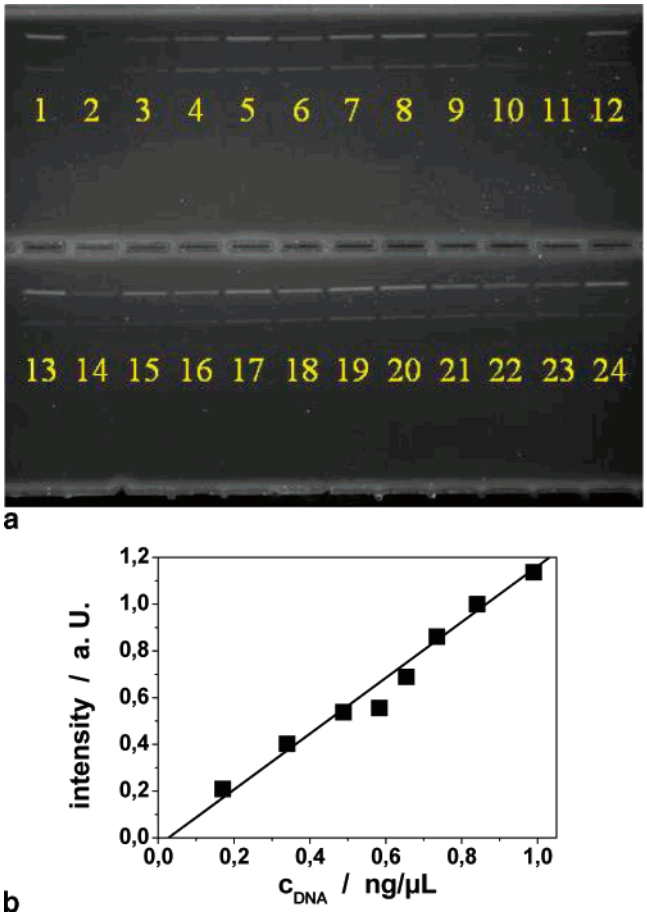

Figure 1. (a) Gel electrophoresis of DNA-PEI-complexes (direction of movement: upward). Samples: (i) Standard ($c_{DNA} = 0.84$ ng mg^{-1}), lane nos. 1, 5, 8, 12, 13, 17, 20, and 24; (ii) uncomplexed DNA with different concentrations (in brackets c_{DNA}), lane nos. 14 (0.17 ng mg^{-1}), 15 (0.41 ng mg^{-1}), 16 (0.58 ng mg^{-1}), 18 (0.73 ng mg^{-1}), 19 (0.99 ng mg^{-1}), 21 (0.65 ng mg^{-1}), 22 (0.49 ng mg^{-1}), and 23 (0.34 ng mg^{-1}); (iii) complex solutions (in brackets mixing ratio w_{DNA} and mass concentration $c_{overall}$), lane nos. 2 (0.60/1.65 ng mg^{-1}), 3 (0.70/1.66 ng mg^{-1}), 4 (0.80/1.13 ng mg^{-1}), 6 (0.90/0.78 ng mg^{-1}), 7 (0.95/0.82 ng mg^{-1}), 9 (0.85/0.82 ng mg^{-1}), 10 (0.75/1.13 ng mg^{-1}), and 11 (0.65/1.65 ng mg^{-1}). (b) Calibration curve (traces ii in Figure 1a) for the quantitative determination of freely migrated DNA in complex solutions as obtained from Figure 1a.

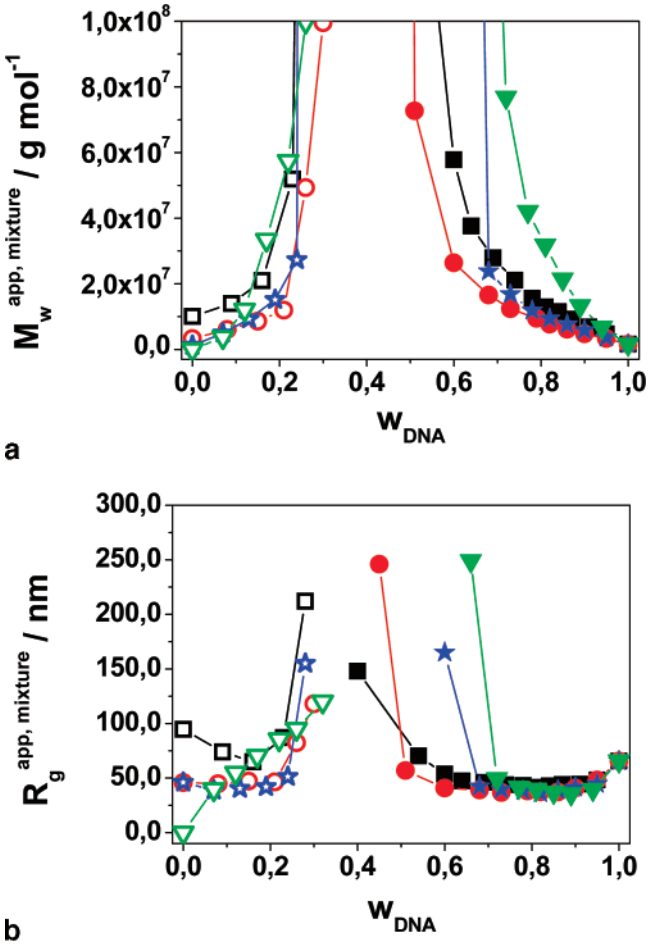

Figure 2. (a) Apparent molar mass as a function of weight fraction w_{DNA} for the various polycation topologies: (■, □) PVP26, (red ●, ○) PVP47, (blue ★,☆) PEI, (green ▼, ▽) PAMAM. Closed symbols: DNA excess and polycation added. Open symbols: polycation excess and DNA added. (b) Apparent radius of gyration as a function of weight fraction w_{DNA} for the various polycation topologies (symbols see Figure 2a).

tion of the respective components and on the mixing protocol, i.e., the sequence and speed of mixing and on even more subtle parameters like stirring speed. Therefore, all complexes in the present work were strictly prepared as described in the Experimental Section.

The complexes formed by supercoiled DNA with various cylindrical brush polymers carrying quaternized polyvinylpyridine or polyethylene imine side chains and with a fifth generation PAMAM dendrimer sample was investigated, thus covering a large regime of molar masses and charge densities besides the different chain topologies, i.e., the cylindrical brushes of different aspect ratios and the spherical dendrimer. A summary of all parameters relevant for complex formation of all samples utilized in the present study is given in Table 2.

In Figure 2a, the apparent molar masses of the respective complexes are plotted as a function of the weight fraction w_{DNA}. The different topologies of the polycations do not seem to have much influence on the results. Also, the usual divergence of

Table 2. Characteristics of the Polycations and of DNA Utilized for Complex Formation

polyion	topology	M_w/g mol^{-1}	size[a]	M_w/M_n	charges/molecule[b] $Z^{+/-}$	charge density[c]
PVP26	cylindrical brush polymer	10.1×10^7	contour length $L_w = 610$ nm	5.3	$\langle Z^+ \rangle_n = 5500$	48 N$^+$/nm
PVP47	cylindrical brush polymer	3.7×10^6	contour length $L_w = 115$ nm	3.9	$\langle Z^+ \rangle_n = 3100$	105 N$^+$/nm
PEI28	cylindrical brush polymer	8.3×10^5 [d,e]	contour length $L_w = 90$ nm	2.7	$\langle Z^+ \rangle_n = 1800$[d]	55 N$^+$/nm
PAMAM-G5	dendrimer	3.8×10^4 [d]	radius $R = 3.4$ nm	~1	$Z^+ = 128$[d]	n. d.
pUC19-supercoiled DNA	supercoiled DNA	1.7×10^6	contour length $L = 930$ nm	1	$Z^- = 5372$	5.9 P$^-$/nm

[a] Weight-average contour length $L_w = P_w \times 0.25$ nm with P_w given by the main chain degree of polymerization. [b] Number-average. [c] Number-average Z_n/L_n. [d] Assuming 100% protonation of the primary amines, 50% of the secondary amines and no protonation of the tertiary amines in phosphate buffer. [e] Value for the hypothetical nonaggregated PEI brush.

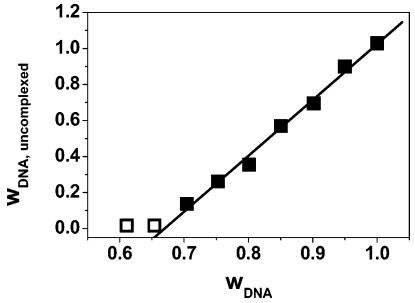

Figure 3. Weight fraction of freely migrated DNA in DNA-PEI complex solutions.

Table 3. Comparison of the Results of Gel Electrophoresis and Light Scattering

polycation	w^*_{DNA}(GE) (gel electrophoresis)	w^*_{DNA}(LS) (light scattering)
PVP26	0.53 ± 0.03	0.54 ± 0.14
PVP47	0.52 ± 0.03	0.51 ± 0.09
PEI28	0.67 ± 0.04	0.68 ± 0.08
PAMAM-G5	0.66 ± 0.07	0.72 ± 0.06

the mass of the complexes is observed if mass or charge stoichiometry is approached. Eventually phase separation/precipitation occurs. The radii of gyration shown in Figure 2b qualitatively confirm this picture. At a high excess of DNA, the polycations are observed to produce even smaller complexes as compared to the size of pure DNA, again almost independent of the polycation topology. Since complexes prepared at small and large w_{DNA} differ considerably, the case of excess DNA is discussed first.

The Regime $w_{DNA} > 0.5$. A closer inspection of Figure 2, parts a and b, reveals the complexes at large excess of DNA, i.e., $0.7 < w_{DNA} < 1$ (the lower limit depending in detail on the respective polycation), to increase in molar mass but to decrease significantly in size as expected for DNA condensation.

For a quantitative picture, it should be known whether the solution contains complexes, only, or complexes coexisting with free DNA.[30−32] For the latter case the fraction of free, i.e., uncomplexed DNA, $w_{DNA,uncomplexed}$, in the respective solutions should be determined quantitatively. Unfortunately, this information is impossible to extract from the light scattering data because the size of the complexes is too close to the size of free DNA. However, gel electrophoresis has been demonstrated to constitute a powerful tool for DNA separations. Figure 1 (see Experimental Section) shows the trace of the complex solutions to exhibit one major band originating from free, uncomplexed DNA. There is no detectable amount of DNA in between the band and the starting point of the samples (except for the weak band of single necked DNA close to the scDNA band[50]). Obviously, the complexed DNA does not migrate at all but is immobilized at the starting point. As a result free DNA is shown to coexist with complexed DNA over a wide regime of w_{DNA}. Moreover, by comparison to the calibration curve shown in the Experimental Section the intensities of the bands may be quantified in order to determine the concentration of free DNA as a function of w_{DNA} as shown in Figure 3 for DNA/PEI complexes (for other polycation complexes, see Supporting Information) and summarized in Table 3. With decreasing w_{DNA} the fraction of free DNA becomes smaller and vanishes at a certain fraction w^*_{DNA}(GE). Remarkably, the decrease is linear, thus showing that the mass fraction of DNA in the complexes formed is constant within experimental error and equal to w^*_{DNA}-(GE) in the regime of mixing ratios $1 > w_{DNA} > w^*_{DNA}$(GE). Additionally, it can be seen that the mass stoichiometry of the complexes w^*_{DNA}(GE) obtained from gel electrophoresis is equal to the composition of the mixture w^*_{DNA}(LS) for which the divergence of the apparent molar mass and the radius of gyration is observed in light scattering as shown in Table 3. Thus, gel electrophoresis and light scattering provide complementary information, which will be used later for data evaluation for the regime $w_{DNA} < 0.5$.

Since the molecular characteristics of free DNA is known by light scattering and its mass fraction is determined by gel electrophoresis the molar masses and dimensions of the pure complexes may be extracted from the light scattering data on the complex solutions according to[51]

$$w_{DNA} + w_{polycation} = w_{DNA,uncomplexed} + w_{complex} = 1 \quad (2)$$

$$\left(\frac{dn}{dc}\right)_{mixture} = w_{DNA,uncomplexed}\left(\frac{dn}{dc}\right)_{DNA} + w_{complex}\left(\frac{dn}{dc}\right)_{complex} \quad (3)$$

$$M_{w,complex} = \frac{\left(\frac{dn}{dc}\right)_{mixture}^2 M_{app,mixture} - w_{DNA,uncomplexed}\left(\frac{dn}{dc}\right)_{DNA}^2 M_{w,DNA}}{w_{complex}\left(\frac{dn}{dc}\right)_{complex}^2} \quad (4)$$

$$\langle R_g^2\rangle_{z,complex} = \frac{\left(\frac{dn}{dc}\right)_{mixture}^2 M_{app,mixture}\langle R_g^2\rangle_{app,mixture}}{w_{complex}\left(\frac{dn}{dc}\right)_{complex}^2 M_{w,complex}} - \frac{w_{DNA,uncomplexed}\left(\frac{dn}{dc}\right)_{DNA}^2 M_{w,DNA}\langle R_g^2\rangle_{z,DNA}}{w_{complex}\left(\frac{dn}{dc}\right)_{complex}^2 M_{w,complex}} \quad (5)$$

$$\langle R_h^{-1}\rangle_{z,complex} = \frac{\left(\frac{dn}{dc}\right)_{mixture}^2 M_{app,mixture}\langle R_h^{-1}\rangle_{app,mixture}}{w_{complex}\left(\frac{dn}{dc}\right)_{complex}^2 M_{w,complex}} - \frac{w_{DNA,uncomplexed}\left(\frac{dn}{dc}\right)_{DNA}^2 M_{w,DNA}\langle R_h^{-1}\rangle_{z,DNA}}{w_{complex}\left(\frac{dn}{dc}\right)_{complex}^2 M_{w,complex}} \quad (6)$$

In the equations above, it is assumed that the effect of the compositional heterogeneity of the complexes can be neglected.

In Figure 4, the molar masses and radii of the complexes are shown together with the complex density defined as

$$\rho_{complex} = 3M_{w,complex}/(N_L 4\pi\langle 1/R_h\rangle_{z,complex}^{-3}) \quad (7)$$

Since R_g/R_h is approximately equal to unity, replacement of R_h by R_g in eq 7 would not affect the complex density within experimental error. As compared to pure DNA ($\rho = 8 \times 10^{-3}$ g cm^{-3}), the density of the complexes increases to about $\rho = 0.2$ g cm^{-3} for all cylindrical brush structures whereas for the PAMAM dendrimer, a somewhat higher density $\rho = 0.3$ g cm^{-3} is observed. It should be noted that the data close to the phase boundary where extensive intercomplex bridging occurs are not significant, because they may be falsified by the very large polydispersity and by the onset of sedimentation of the largest particles during the time of the scattering measurements.

On the basis of the results shown in Figure 4a−c, it is safe to conclude that in the initial phase of polycation addition, which is characterized by constant molar masses and radii of the

Table 4. Mass and Charge Stoichiometry of the Primary Complexes and Weight Average Number of DNA and Polycation Molecules Incorporated in One Primary Complex: Excess DNA

polycation	no. of DNA molecules/complex	no. of polycations/complex	mass stoichiometry w^*_{DNA}(GE)	charge stoichiometry N^+/P^-
PVP26	9.2 ± 0.5	7.1 ± 0.5	0.53 ± 0.03	0.79 ± 0.1
PVP47	5.0 ± 0.3	8.5 ± 0.6	0.52 ± 0.03	0.98 ± 0.1
PEI28	6.1 ± 0.4	16 ± 2	0.67 ± 0.04	0.87 ± 0.2
PAMAM-G5	10 ± 1	310 ± 70	0.66 ± 0.07	0.73 ± 0.2

Table 5. Mass and Charge Stoichiometry of the Primary Complexes and Average Number of DNA and Polycation Molecules Incorporated in One Primary Complex: Excess Polycation

polycation	no. of DNA molecules/complex	no. of polycations/complex	mass stoichiometry w^{**}_{DNA}(LS)	charge stoichiometry N^+/P^-
PVP26	3.2 ± 0.4	9.4 ± 1.2	0.23 ± 0.05	3.0 ± 0.8
PVP47	2.7 ± 0.2	11.3 ± 1	0.30 ± 0.05	2.4 ± 0.6
PEI28	2.4 ± 0.3	41 ± 6	0.24 ± 0.05	5.6 ± 1.5
PAMAM-G5	3.2 ± 1.1	410 ± 110	0.32 ± 0.06	2.9 ± 0.8

Table 6. Mass Stoichiometry of the Primary Complexes and Average Number of DNA and PVP26 Molecules Incorporated in One Primary Complex as a Function of the Concentration of Mixing

excess component	c_{DNA}/mg L^{-1}	c_{PVP26}/mg L^{-1}	mass stoichiometry w^*_{DNA} or w^{**}_{DNA}	no. of DNA molecules/complex	no. of PVP26 molecules/complex
DNA	2.5	2.5	0.54 ± 0.14	9.2 ± 0.5	7.1 ± 0.5
DNA	25	25	0.53 ± 0.05	36 ± 2	28 ± 2
DNA	25	100	0.56 ± 0.10	160 ± 30	110 ± 20
PVP26	2.5	2.5	0.23 ± 0.05	3.2 ± 0.4	9.4 ± 1.2
PVP26	25	25	0.26 ± 0.05	19 ± 5	47 ± 13
PVP26	100	25	0.29 ± 0.06	50 ± 7	110 ± 10

complexes, only primary complexes are being formed. At smaller fractions w_{DNA} the number of complexes becomes comparable to the number of uncomplexed molecules and accordingly inter complex bridging becomes more and more significant which eventually leads to phase separation.

The statements above hold true for all cylindrical brush−DNA complexes, whereas for the PAMAM dendrimer the situation is not so clear. As compared to the cylindrical brush complexes the initial phase of exclusive primary complex formation is extremely small. It is not even clear that the equivalent of primary complexes exists for the PAMAM system since molar masses and radii immediately start to increase even at the largest excess of DNA investigated. Since the dendrimer and the PEI brushes are chemically similar the onset of

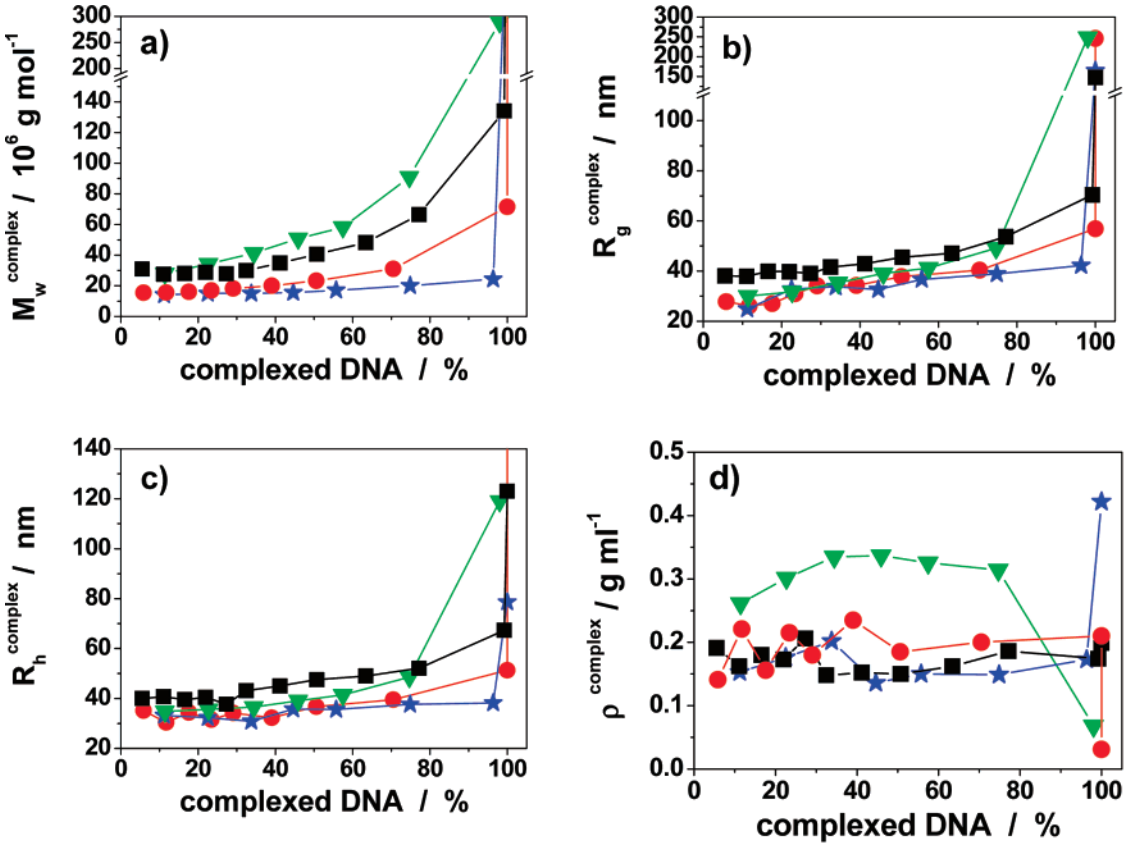

Figure 4. Molar masses (a), radii of gyration (b), and hydrodynamic radii (c) and densities (d) of the complexes as a function of the complexed DNA fraction for the various polycations: (■) PVP26; (red ●) PVP47; (blue ★) PEI; (green ▼) PAMAM.

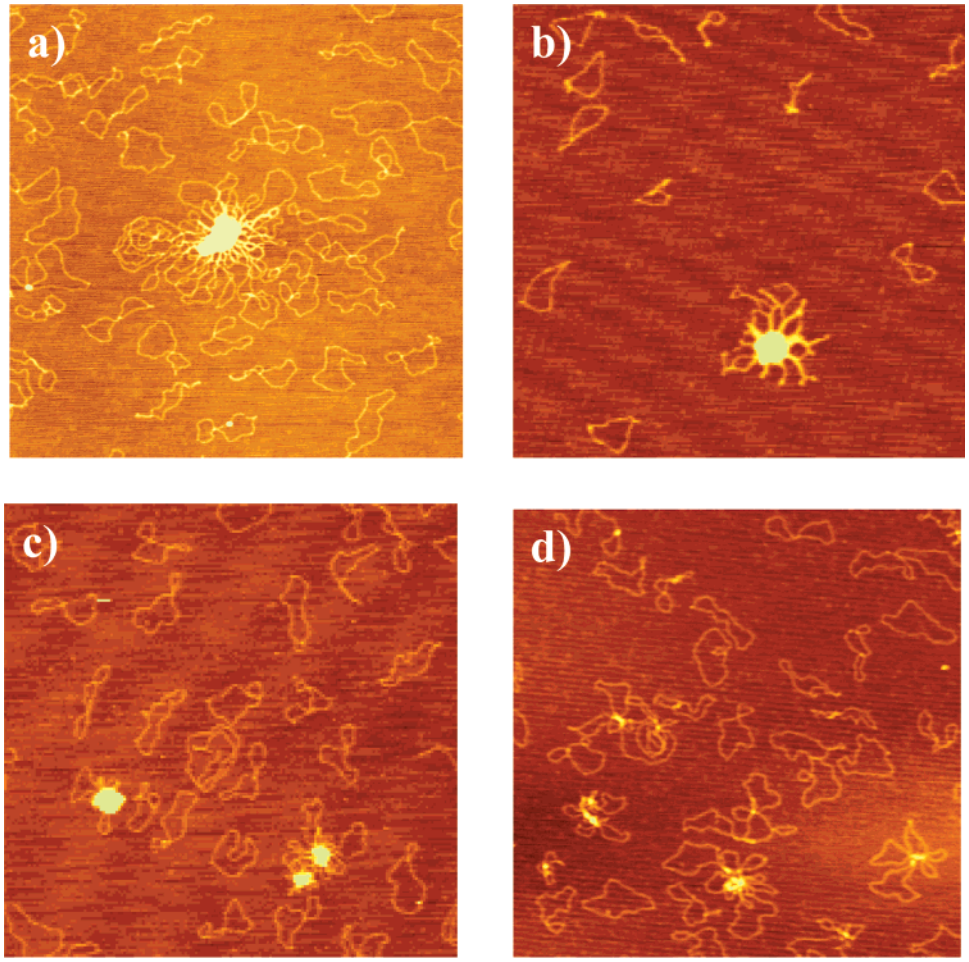

Figure 5. AFM pictures of various DNA/Polycation complexes: (a) DNA/PVP26 complexes ($w_{DNA} = 0.80$; $w_{DNA,uncomplexed} = 0.58$); (b) DNA/PVP47 complexes ($w_{DNA} = 0.75$; $w_{DNA,uncomplexed} = 0.47$); (c) DNA/PEI complexes ($w_{DNA} = 0.80$; $w_{DNA,uncomplexed} = 0.40$); (d) DNA/PAMAM complexes ($w_{DNA} = 0.90$; $w_{DNA,uncomplexed} = 0.68$). The size of all AFM pictures is 2×2 μm.

secondary complex formation seems not to be correlated with the chemical nature or the charge density, but rather with the absolute molar mass or with the topology of the polycations.

At this point a clear terminology should be introduced. A "primary complex" is formed under the condition of a large excess of free DNA.[52] Under "secondary complexes" all complexes are summarized which develop by inter complex formation of primary complexes. The term "complex solution" refers to the solution containing primary and possibly secondary complexes and free DNA. The data on "pure complexes" originate from primary and possibly secondary complexes, only, i.e., the possible contribution of free DNA has been eliminated as described below.

Since the molar mass and the DNA content of the complexes are known it is elucidating to calculate the absolute weight-average number N_w of DNA and polycation chains within one respective complex by

$$N_{w,chains}(X) = \frac{w_{X,complex} M_{w,complex}}{M_{n,X}} \quad (8)$$

with X being either DNA or polycation. For the polydisperse polycations $M_n(X)$ has to be utilized rather than $M_w(X)$. The latter would yield $N_{w,w,chains}$, which is difficult to interpret.

The results are listed in Table 4 and reveal most interesting although puzzling differences. The most important observation is that the composition of all primary complexes is governed by the net charge which is not zero but slightly negative for all complexes formed at excess DNA independent of polycation topology. The slight overcharging of the polycations by the excess DNA chains lies in the range known for soluble polyelectrolyte polyelectrolyte complexes.[3,4,6,14]

The number of DNA helices in one primary complex varies between 5 and 10, again not correlated to any obvious polycation property. The number of polycations per primary complex increases from 7 to 310 as the polycation molar mass decreases.

The structure and size of the primary complexes do not seem to be significantly influenced by the polycation topology. This hypothesis is confirmed by AFM micrographs of the complex solutions shown in Figure 5. Although the significance of the AFM pictures is somewhat limited by the fact that $MgCl_2$ was added in order to improve the interaction of DNA with the mica surface leading to better pictures and that the complexes were transferred into a two-dimensional dry film, the pictures seem to reveal that DNA encapsulates the polycations in a highly heterogeneous manner. For all complexes—and even for the PAMAM dendrimer complexes—a core comprising at least several complexed polycation molecules is surrounded by an open DNA corona resulting in a flower-like structure. Assuming that the sample preparation does not significantly alter the complex topology and composition, the density of the core must be quite high given the large overall complex density determined by light scattering (see Figure 4d). It is interesting to note the effect of charge density mismatch, i.e., the vastly different chemical charges per unit length between DNA (5.9 P^-/nm) and the cylindrical brush polymers (from 48 to 105 N^+/nm). It

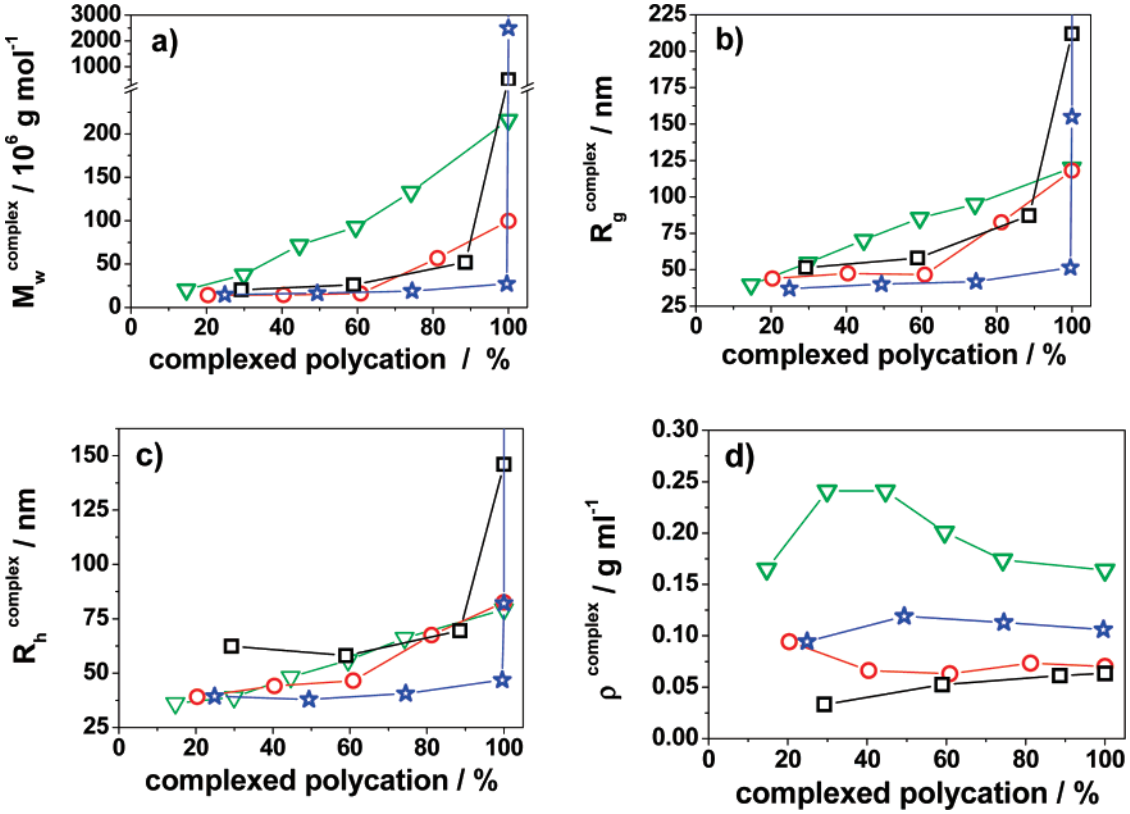

Figure 6. Molar masses (a), radii of gyration (b), and hydrodynamic radii (c) and densities (d) of the complexes as a function of the complexed polycation fraction: (□) PVP26; (red ○) PVP47; (blue ☆) PEI; (green ▽) PAMAM.

follows from simple geometric considerations that a single layer of DNA molecules arranged around a cylindrical brush molecule is not able to compensate the cationic charges, and accordingly, the effective charge of the densely packed core must remain positive, if charge compensation by bound counterions, i.e., ion pair formation/condensation, does not occur.[42] Unlike in Gössel et al.,[40,41] no single brush−DNA complex could be identified in order to examine the reduction of the DNA contour length and elucidate the local structure of the complexes.

Complexes formed at w_{DNA} < 0.5. At excess of polycations a qualitatively similar behavior is observed. As seen in Figure 2 and summarized in Table 5, the divergence of the molar masses occurs already at w^{**}_{DNA}(LS) as small as 0.23 < w^{**}_{DNA}(LS) < 0.32 (w^{**}_{DNA} is introduced in order to avoid confusion with the critical DNA fraction at DNA excess, w^{*}_{DNA}), depending in detail on the polycation utilized. Unfortunately, gel electrophoresis could not yet be established for the polycations in order to quantify the fraction of free polycations coexisting with the complexes. Although alternative methods like AFM or GPC[30] may also be utilized as shown for one representative example (see Supporting Information), these techniques were not applied to all samples investigated in this work because they are not very reliable. AFM is not an ensemble averaging method, and GPC requires the complex solution to be concentrated by at least a factor of 100 and no adsorption of the complexes on the column to occur. Therefore, the evaluation of the light scattering data in terms of the structure of the primary complexes required the following two assumptions:

•As for the case of excess DNA (see Table 3), the onset of the divergence of the molar masses indicates significant intercomplex bridging to occur; i.e., below this weight fraction w^{**}_{DNA} primary and secondary complexes are assumed to coexist with free polycation.

•The mass fraction of free polycations decreases linearly with increasing w_{DNA} in strict analogy to the experimental results obtained from the complexation in the regime of excess DNA.

Since both assumptions were proven to be fulfilled for complexation of DNA by excess PVP47 (see Supporting Information) it is quite conceivable that they also hold true for the other polycations investigated in the present study. As a result characterization of the primary complexes formed by DNA and excess polycations is shown in Figure 6, parts a−c, along with the corresponding densities (Figure 6d). Again, the size of the primary complexes does not vary much for the cylindrical brush polycations, whereas for the PAMAM dendrimers a monotonous increase in size is observed even for the largest excess of dendrimer investigated. Therefore, the complexation with dendrimers might not lead to strictly defined primary complexes as already discussed for the regime with excess DNA.

The density of the primary complexes is only half as large as for those formed by excess DNA. As above, the mass and the charge stoichiometry as well as the mean number of polycation and DNA molecules per primary complex may be calculated, and the results are summarized in Table 5.

The number of DNA molecules per complex is significantly smaller than observed for complexes formed by excess DNA, whereas the number of polycation molecules in one complex is slightly smaller thus resulting in a very different net charge of the primary complexes of as high as $N^+/P^- \approx 3$ for PVP26, PVP47, and PAMAM-G5 or $N^+/P^- \approx 6$ for PEI. The increased cationic excess charge for PEI complexes as compared to the PVP brushes could be confirmed for complexes with poly(styrenesulfonate) brushes,[53] thus representing a highly interesting detail which is not yet understood. For any polycation utilized in the present work, the charge stoichiometry N^+/P^- at excess polycation not only is in contrast to the small excess of

Scheme 1. Illustration of the Charge Mismatch for Complexes of DNA and Cylindrical Brushes. Left: DNA Excess. Right: Brush Excess.

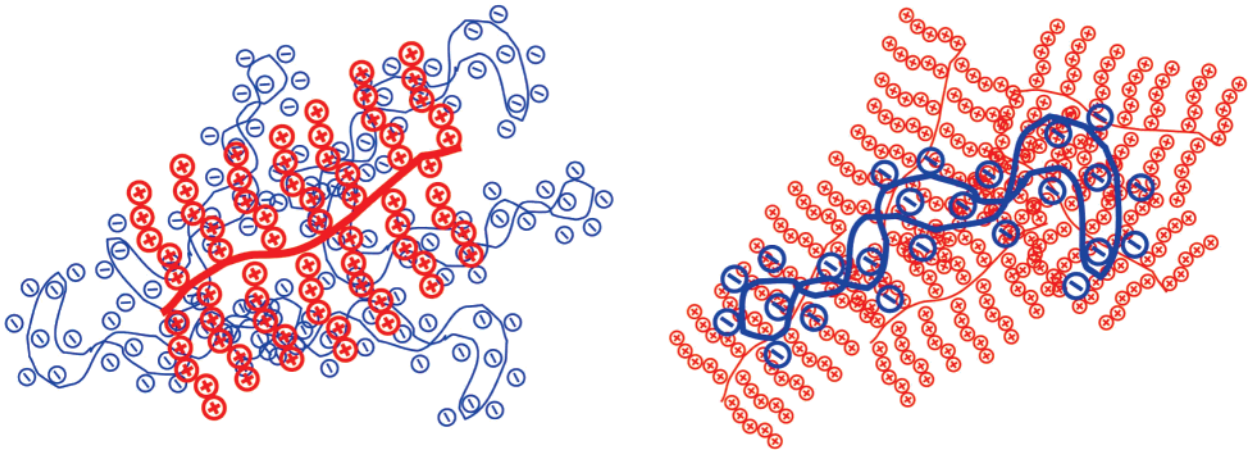

anionic charges of the complexes formed in the presence of excess DNA but also is much higher than $N^+/P^- = 1.25$ reported for complexes of DNA and linear flexible PEI chains.[30] Obviously the extreme mismatch of the linear charge densities of the polycations utilized in the present study and DNA results in highly overcharged complexes, if the excess component, i.e., the cylindrical brush polymers (and the PAMAM dendrimers) exhibit the higher charge density.

Effect of Concentration of Mixing. So far, the complex formation was investigated for extremely low concentrations of both components. In particular, it is not clear whether or not the formation of primary complexes in the regime of a large excess of either of the two components does also occur at higher concentrations. In order to clarify this point, some preliminary measurements were conducted utilizing higher concentrations. The light scattering results are shown in the Supporting Information and are summarized in Table 6. Besides the formation of larger complexes due to the increased concentrations, the charge stoichiometry of the primary complexes remains constant, thus demonstrating that the picture of complex formation derived from the results above is valid over a wider concentration range.

Conclusion

As expected and postulated in the literature, the complex formation of DNA with polycations of various chain topologies is kinetically controlled and depends in a subtle manner on parameters like the concentration, speed and sequence of mixing. Apparently, the initial growth of the complexes is diffusion-controlled until a certain net charge of the complexes is reached where the complexes do not grow anymore (primary complexes) and coexist with the molecules of the excess component. Upon further addition of the minority component, preferentially new complexes are being formed as long as the number of primary complexes is small as compared to the number of uncomplexed molecules of the excess component. Only if the number of primary complexes becomes comparable to the number of free polyions does bridging between primary complexes become more and more probable, thus leading to intercomplex formation and eventually to precipitation/phase separation.

More specifically, the results demonstrate the influence of charge density mismatch between DNA and the polycations on the complex properties as sketched in Scheme 1. For the highly charged cylindrical brush polycations, the locally formed complexes, i.e., those involving a cylindrical brush and a small part of the DNA, exhibit a large cationic excess charge that cannot be compensated by extensive backfolding of the same DNA molecule. As more and more DNA molecules participate in one complex, the cationic core is surrounded by a corona of anionically charged DNA loops thus protecting the cationic core against further complexation. These primary complexes appear to be stabilized electrostatically and/or sterically if a slight excess of anionic charges of the whole complex is reached, i.e., 20% amounting to approximately 8000 excess anionic charges out of a total of 40 000 anionic charges per primary complex.

A qualitatively similar but quantitatively different scenario is envisioned if DNA is added to an excess of the much higher charged polycations. Again, at the location of complex formation an extremely high cationic charge persists locally. Because of the kinetically controlled complexation process the same DNA molecules may be complexed by more than one polycation at different positions along its contour which become electrostatically shielded against further polycation complexation at a much higher net cationic charge of the primary complexes, i.e., approximately 40 000 excess cationic charges out of a total of 50 000 cationic charges per complex.

On the basis of the scenarios described above the present work might provide new guidelines for the preparation of DNA−polycation complexes of any size and cationic charge: The number of DNA molecules in one complex is governed by the dilution during mixing whereas the net charge of the complex is controllable by the charge density mismatch between DNA and the polycation.

Future work is needed to further experimentally substantiate the hypothesis above and to resolve more subtle details such as the meaning of the term “charge density”. So far the charge density was pragmatically defined as the number of chemical charges of a polyion which is known to differ dramatically from the “effective charges”. Little is known so far about the effective charge of the complex polycations utilized in the present work.

Finally, the results of the present work raise many more questions, particularly if related to the published literature on highly ordered structures of DNA complexes and various polycations in the dry state.[54−56] The “scrambled egg” or “flowerlike” complexes observed in the present work have been reported in the literature as well,[57,58] and it is not entirely clear how complexation may be directed toward ordered structures such as rods or toroids. In general, the latter structures may be preferably (but not exclusively) formed at high ionic strength[57,59] and/or with small cations.[58,60−63] Since structural rearrangements during drying can also not be entirely excluded further more detailed investigations in solution seem to be necessary.

Acknowledgment. This work was supported by the "Deutsche Forschungsgemeinschaft" (SFB 625). Two of us (D. S. and S. D.) are grateful to the International Max Planck Research School "Polymers in Advanced Materials", Mainz, Germany, for financial support. We are indebted to Dr. Tim Stephan for providing us with the cylindrical brush polymers with quaternized polyvinylpyridinium side chains. Fruitful and stimulating discussions with Prof. M. Muthukumar, Department of Polymer Science, University of Massachusetts, Amherst, MA, are gratefully acknowledged as well as the practical advice of Prof. E. Schmidt, Institute of Genetics, Mainz, Germany.

Supporting Information Available: Figures showing a Berry plot of the pUC19 DNA, gel electrophoresis results of complexes with PVP26, PVP47, and PAMAM, determination of the amount of uncomplexed PVP47 in complex solutions formed at excess PVP47, and concentration dependence of the molar mass of the complex solution with PVP26 for different compositions. This material is available free of charge via the Internet at http://pubs.acs.org.

References and Notes

(1) Wieland, T.; Goldmann, H.; Kern, W.; Schultze, N. E.; Matheka, H. D. *Makromol. Chem.* **1953**, *10*, 136−146.
(2) Michaels, A. S.; Miekka, R. G. *J. Phys. Chem.* **1961**, *65*, 1765.
(3) Kabanov, V. A.; Zezin, A. B.; Izumrudov, V. A.; Bronich, T. K.; Bakeev, K. N. *Makromol. Chem. Suppl.* **1985**, *13*, 137−155.
(4) Dautzenberg, H. *Macromol. Symp.* **2000**, *162*, 1.
(5) Thünemann, A. F.; Müller, M.; Dautzenberg, H.; Joanny, J. F.; Löwen, H. *Adv. Polym. Sci.* **2004**, *166*, 113−171.
(6) Karibyants, N.; Dautzenberg, H.; Cölfen, H. *Macromolecules* **1997**, *30*, 7803.
(7) Zinchenko, A. A.; Chen, N. *J. Phys.: Condens. Matter* **2006**, *18*, R453.
(8) Bloomfield, V. A. *Biopolymers* **1997**, *44*, 269.
(9) Park, T. G.; Jeong, J. H.; Kim, S. W. *Adv. Drug. Del. Rev.* **2006**, *58*, 467.
(10) Haag, R.; Kratz, F. *Angew. Chem., Int. Ed.* **2006**, *45*, 1198.
(11) Vijayanathan, V.; Thomas, T.; Thomas, T. J. *Biochemistry* **2002**, *41*, 14085.
(12) Godbey, W. T.; Mikos, A. G. *J. Controlled Release* **2001**, *72*, 115.
(13) Luo, D.; Saltzman, W. M. *Nat. Biotechnol.* **2000**, *18*, 33.
(14) Kabanov, A. V.; Kabanov, V. A. *Bioconjugate Chem.* **1995**, *6*, 7.
(15) Bronich, T.; Kabanov, A. V.; Marky, L. A. *J. Phys. Chem. B* **2001**, *105*, 6042.
(16) Nguyen, H-K.; Lemieux, P.; Vinogradov, S. V.; Gebhart, C. L.; Guerin, N.; Paradis, G.; Bronich, T. K.; Alakhov, V. Y.; Kabanov, A. V. *Gene Ther.* **2000**, *7*, 126.
(17) Gebhart, C. L.; Sriadibhatla, S.; Vinogradov, S.; Lemieux, P.; Alakhov, V.; Kabanov, A. V. *Bioconjugate Chem.* **2002**, *13*, 937.
(18) Gebhart, C. L.; Kabanov, A. V. *J. Controlled Release* **2001**, *73*, 401.
(19) Bronich. T. K.; Nguyen, H. K.; Eisenberg, A.; Kabanov, A. V. *J. Am. Chem. Soc.* **2000**, *122*, 8339.
(20) Fischer, D.; Dautzenberg, H.; Kunath, K.; Kissel, T. *Int. J. Pharmaceutics* **2004**, *280*, 253.
(21) Akagi, D.; Oba, M.; Koyama, H.; Nishiyama, N.; Fukushima, S.; Miyata, T.; Nagawa, H.; Kataoka, K. *Gene Ther.* **2007**, *14*, 1029.
(22) Katayose. S.; Kataoka, K. *Bioconjugate Chem.* **1997**, *8*, 702.
(23) Katakura, H.; Harada, A.; Kataoka, K.; Tanaka, F.; Wada, H.; Ikenaka, K. *J. Gene Med.* **2004**, *6*, 471.
(24) Oupicky, D.; Reschel, T.; Konak, C.; Oupicka, L. *Macromolecules* **2003**, *36*, 6863.
(25) Bisht, H. S.; Manickam, D. S.; You, Y.; Oupicky, D. *Biomacromolecules* **2006**, *7*, 1169.
(26) Wolfert, M. A.; Dash, P. R.; Nazarova, O.; Oupicky, D.; Seymour, L. W.; Smart, S.; Strohalm, J.; Ulbrich, K. *Bioconjugate Chem.* **1999**, *10*, 993.
(27) Putnam, D.; Zelikin, A. N.; Izumrudrov, V. A.; Langer, R. *Biomaterials* **2003**, *24*, 4425.
(28) DeRouchey, J.; Walker, G. F.; Wagner, E.; Rädler, J. O. *J. Phys. Chem. B* **2006**, *110*, 4548.
(29) Ogris, M.; Steinlein, P.; Kursa, M.; Mechtler, K.; Kircheis, R.; Wagner, E. *Gene Ther.* **1998**, *5*, 1425.
(30) Boeckle, S.; von Gersdorff, K.; van der Piepen, S.; Culmsee, C.; Wagner, E.; Ogris, M. *J. Gene Med.* **2004**, *6*, 1102.
(31) Clamme, J. P.; Azoulay, J.; Mély, Y. *Biophys. J.* **2003**, *84*, 1960.
(32) Koetz, J.; Koepke, H.; Schmidt-Naake, G.; Zarras, P.; Vogl, O. *Polymer* **1996**, *37*, 2775−2781.
(33) Mitra, A.; Imae, T. *Biomacromolecules* **2004**, *5*, 69.
(34) Kabanov, V. A.; Sergeyev, V. G.; Pyshkina, O. A.; Zinchenko, A. A.; Zezin, A. B.; Joosten, J. G. H.; Brackman, J.; Yoshikawa, K. *Macromolecules* **2000**, *33*, 9587.
(35) Chen, W.; Turro, N. J.; Tomalia, D. A. *Langmuir* **2000**, *16*, 15−19.
(36) Ottaviani, M. F.; Sacchi, B.; Turro, N. J.; Chen, W.; Jockush, S.; Tomalia, D. A. *Macromolecules* **1999**, *32*, 2275.
(37) Ottaviani, M. F.; Furini, F.; Casini, A.; Turro, N. J.; Jockusch, S.; Tomalia, D. A.; Messori, L. *Macromolecules* **2000**, *33*, 7842.
(38) Zinchenko, A. A.; Yoshikawa, K.; Baigl, D. *Phys. Rev. Lett.* **2005**, *95*, 228101.
(39) Keren, K.; Soen, Y.; Yoseph, G. B.; Gilad, R.; Braun, E.; Sivan, U.; Talmon, Y. *Phys. Rev. Lett.* **2002**, *89*, 088103.
(40) Gössl, I.; Shu, L.; Schlüter, A. D.; Rabe, J. P. *J. Am. Chem. Soc.* **2002**, *124*, 6860.
(41) Gössl, I.; Shu, L.; Schlüter, A. D.; Rabe, J. P. *Single Molecules* **2002**, *3*, 315.
(42) Rühe, J.; Ballauff, M.; Biesalski, M.; Dziezok, P.; Gröhn, F.; Johannsmann, D.; Houbenov, N.; Hugenberg, N.; Konradi, R.; Minko, S.; Motornov, M.; Netz, R. R.; Schmidt, M.; Seidel, C.; Stamm, M.; Stephan, T.; Usov, D.; Zhang, H. *Adv. Polym. Sci.* **2004**, *165*, 79.
(43) Fishman, D.; Patterson, G. *Biopolymers* **1996**, *38*, 535.
(44) Jolly, D.; Eisenberg, H. *Biopolymers* **1976**, *15*, 61.
(45) Gross, A.; Maier, G.; Nuyken, O. *Macromol. Chem. Phys.* **1996**, *197*, 2811.
(46) Tanaka, R.; Ueoka, I.; Takaki, Y.; Kataoka, K.; Saito, S. *Macromolecules* **1983**, *16*, 849.
(47) Smits, R. G.; Koper, G. J. M.; Mandel, M. *J. Phys. Chem.* **1993**, *97*, 5745.
(48) Park, I. H.; Choi, E. *Polymer* **1996**, *37*, 313.
(49) Becker, A.; Köhler, W.; Müller, B. *Ber. Bunsen-Ges. Phys. Chem.* **1995**, *99*, 600.
(50) One reviewer has noticed that the intensity ratios between the supercoiled and single necked DNA bands are different for the complex traces as compared to the pure DNA traces shown in Figure 1a. Although this effect is too small in order to be quantified in the present work, it may point towards the possibility of a preferred complexation of supercoiled DNA as postulated in the literature for supercoiled vs linear DNA: Bronich, T. K.; Nguyen, H. K.; Eisenberg, A.; Kabanov, A. V. *J. Am. Chem. Soc.* **2000**, *122*, 8339.
(51) Benoit, H.; Froelich, D. In *Light Scattering from Polymer Solutions*; Huglin, M. B., Ed. Academic Press: London and New York, 1972; Chapter 11.
(52) It should be noted that this global description does not properly characterize the precise condition at which the complexes locally form when the first droplet of minority component falls into the solution of the excess component.
(53) Unpblished results.
(54) Evans, H. M.; Ahmad, A.; Ewert, K.; Pfohl, T.; Martin-Herranz, A.; Bruinsma, R. F.; Safinya, C. R. *Phys. Rev. Lett.* **2003**, *91*, 075501.
(55) Golan, R.; Pietrasanta, L. I.; Hsieh, W.; Hansma, H. G. *Biochemistry* **1999**, *38*, 14069.
(56) Liu, Y-C.; Chen, H-L.; Su, C-J.; Lin, H-J.; Liu, W-L.; Jeng, U-S. *Macromolecules* **2005**, *38*, 9434.
(57) Hansma, H. G.; Golan, R.; Hsieh, W.; Lollo, C. P.; Mullen-ley, P.; Kwoh, D. *Nucleic Acids Res.* **1998**, *26*, 2481.
(58) Fang, Y.; Hoh, J. H. *J. Am. Chem. Soc.* **1998**, *120*, 8903.
(59) Golan, R.; Pietrasanta, L. I.; Hsieh, W.; Hansma, H. G. *Biochemistry* **1999**, *38*, 14069.
(60) Arscott, P. G.; Li, A-Z.; Bloomfield, V. A. *Biopolymers* **1990**, *30*, 619.
(61) Hud, N. V.; Downing, K. H. *Proc. Natl. Acad. Sci. U.S.A.* **2001**, *98*, 14925.
(62) Vijayanathan, V.; Thomas, T.; Antony, T.; Shirahata, A.; Thomas, T. J. *Nucleic Acids Res.* **2004**, *32*, 127.
(63) Lin, Z.; Wang, C.; Feng, X.; Liu, M.; Li, J.; Bai, C. *Nucleic Acids Res.* **1998**, *26*, 3228.

MA0711689